Nonlinear Waves.
Solitons. Autowaves. Self-Organization

Izvestiya Vysshikh Uchebnykh Zavedeniy. Applied Nonlinear Dynamics. 2024;32(3)

Article DOI: 10.18500/0869-6632-003104

Detection of focused beams of surface magnetostatic waves in YIG / Pt structures

M. E. Seleznev[1,2]✉, *G. M. Dudko*[1], *Y. V. Nikulin*[1,2], *Y. V. Khivintsev*[1,2], *V. K. Sakharov*[1,2], *A. V. Kozhevnikov*[1], *S. L. Vysotskii*[1,2], *Y. A. Filimonov*[1,2]

[1]Saratov Branch of Kotelnikov Institute of Radioengineering and Electronics of the RAS, Russia
[2]Saratov State University, Russia
E-mail: ✉mixanich94@mail.ru, dugal_2010@hotmail.com, yvnikulin@gmail.com, khivintsev@gmail.com, valentin@sakharov.info, kzhavl@gmail.com, vysotsl@gmail.com, yuri.a.filimonov@gmail.com
Received 13.12.2023, accepted 2.02.2024, available online 10.04.2024, published 31.05.2024

Abstract. The *purpose* of this work is to experimentally study, using the inverse spin Hall effect (ISHE), the detection of focused beams of magnetostatic surface waves (MSSW) in integrated YIG (3.9 μm) / Pt (4 nm) thin-film microstructures, where the focusing effect was ensured by the curvilinear shape of the exciting antenna. Make a comparison with the case of detecting MSSWs excited by a rectilinear antenna. *Methods.* Experiments were carried out using the delay line structures based on the YIG/Pt. The amplitude-frequency characteristics of the YIG/Pt structure and the frequency dependence of the EMF ($V(f)$) induced in platinum were studied. *Results.* It was shown that at frequencies f near the long-wavelength limit of the MSSW spectrum, the magnitude of the EMF $V(f)$ generated by a focused MSSW can be several times higher than the values of $V(f)$ in the case of MSSW excitation by a common (straight) antenna. In this case, in the short-wavelength part of the spectrum, on the contrary, the magnitude of the EMF generated by the focused MSSW beam turns out to be noticeably smaller. This behavior is associated with chromatic aberration of the focusing antenna for the MSSW, which manifests itself in the frequency dependence of the focal length of the antenna, which is confirmed by the results of micromagnetic modeling. It is shown that the drop in the EMF signal generated by a focused MSSW beam in the short-wavelength part of the spectrum is associated with the focus reaching the area of the YIG not covered with the Pt film. In this case, the increase in $V(f)$ in the long-wavelength region of the MSSW spectrum is explained by an increase in the linear power density of the MSSW and the formation of caustics under the Pt film. *Conclusion.* Obtained results can be used for the development of highly sensitive spin wave detectors and the creation of spin logic devices.

Keywords: YIG / Pt structures, focusing antennas, magnetostatic surface waves, inverse spin Hall effect, micromagnetic modeling.

Acknowledgements. The work was supported by RSF grant No. 22-19-00500.

For citation: Seleznev ME, Dudko GM, Nikulin YV, Khivintsev YV, Sakharov VK, Kozhevnikov AV, Vysotskii SL, Filimonov YA. Detection of focused beams of surface magnetostatic waves in YIG / Pt structures. Izvestiya VUZ. Applied Nonlinear Dynamics. 2024;32(3):405–418. DOI: 10.18500/0869-6632-003104

Introduction

The problems of generation, transfer and detection of spin currents (electron angular momentum currents) are key for spintronics [1–7]. At the same time, of particular interest from the point of view of developing an energy-efficient element base are structures based on yttrium iron garnet (YIG) and platinum (Pt) films, where the spin current can be transferred by spin waves (SW) without the participation of charge motion. The effects of SW propagation and interference in magnetic microstructures can be used to build energy-efficient logic devices [8,9], as well as for special data processing - pattern recognition [10, 11], prime factorization [12], magnetic particle visualization [13], spectral analysis [14]. Computational algorithms are also being developed that use the formation of an interference pattern between coherent wavefronts to implement non-Boolean computations [10, 11, 15–18] and methods for processing magnetic images based on the principles of spin-wave Fourier optics [19].

The implementation of such functional spin-wave information processing devices can be based on the principles of spin-wave optics. This involves the integration of spin-wave optics elements (prisms, lenses, mirrors, splitters) with magnetic films [17–22]. In this case, the problem of integrating spin-wave emitters and receivers with magnetic films, capable of effectively generating and detecting directed beams of spin waves formed without geometric restrictions on the waveguide medium, becomes relevant. For this purpose, point sources of spin waves [17,23–28] and specially designed spin wave focusing antennas [21,29–32] can be used.

In YIG/Pt spintronic structures, methods based on the generation and detection of spin current can be used to excite and detect spin waves [3–7]. In such structures, mutual conversion of spin and electric currents can be realized due to the effects of electron-magnon scattering at the YIG/Pt interface [33]. In this case, a constant electric current in the platinum film can lead to the generation of spin waves due to the spin Hall effect [33, 34], and due to the inverse spin Hall effect, the spin current can be converted back into electric current [33, 35]. Until now, spin wave detection using the inverse spin Hall effect has been studied by excitation of spin waves by rectilinear microstrip antennas, when spin wave focusing effects were absent [36–43]. The aim of this work is to study the detection of focused beams of magnetostatic surface waves (MSSW) in YIG/Pt structures.

The design of spin wave focusing antennas depends on the nature of spin wave dispersion. Focusing elements for spin waves with isotropic dispersion (forward bulk spin waves in a normally magnetized ferrite film) have a concave shape relative to the focus [21] by analogy with traditional optics. In contrast, for waves with anisotropic dispersion (magnetostatic surface waves or backward bulk magnetostatic waves) in tangentially magnetized films, the shape of the focusing elements is convex [21, 32]. In this paper, we investigate the detection of magnetostatic surface wave beams in a YIG/Pt structure focused using a curvilinear microstrip antenna. We compare the detection efficiency of magnetostatic surface waves excited by curvilinear and rectilinear antennas.

1. The structure under study and the experimental methodology

The experiments were performed with YIG/Pt structures of the magnetostatic surface wave delay line type, their micrograph is shown in Fig. 1, *a*. The structures were formed on the surface of a YIG film with a thickness of $d_{YIG} \approx 3.9$ μm, saturation magnetization of $4\pi M_0 \approx 1750$ G, epitaxially grown on a gadolinium gallium garnet substrate with a crystallographic orientation (111). Pairs of antennas (1 and 2) with contact pads for connecting microwave microprobes were formed on the surface of the YIG film using magnetron sputtering, photolithography and ion etching, between which there was an area covered with a Pt film. One of the antennas had the

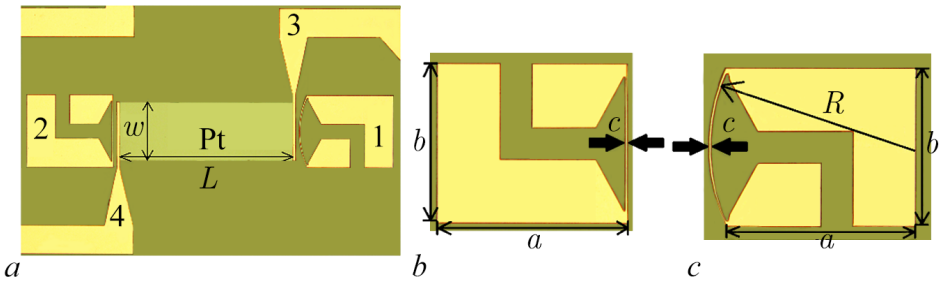

Fig 1. *a* — The delay line structure for MSSW on the base of YIG/Pt sample where 1 and 2 — a pair of antennas for MSSW excitation and reception, 3 and 4 — contacts for EMF measurement in Pt film with the length $L = 620$ μm and width $w = 200$ μm; *b* — the form of straight-line antenna with the aperture $b = 250$ μm and width $c = 4$ μm, the length of the contact pad $a = 300$ μm; *c* — the form of curvilinear antenna with the aperture $b = 250$ μm, width $c = 4$ μm and radius of curvature $R = 300$ μm, the length of the contact pad $a = 300$ μm

shape of a straight microstrip with a length of $a = 300$ μm, aperture $b = 250$ μm and width $c = 4$ μm (Fig. 1, *b*). The other antenna was focusing and had a curved shape convex towards the Pt film with a curvature radius of $R = 300$ μm, aperture $b = 250$ μm and width $c = 4$ μm (Fig. 1, *c*). The shape of the focusing antenna was calculated using the method described in [44]. The platinum film had a length of $L = 620$ μm, a width of $w = 200$ μm and a thickness of $d_{\text{Pt}} = 4$ nm. Copper contacts (3 and 4) were made to the platinum film to measure the electromotive force V generated in platinum due to the inverse spin Hall effect. The model was placed in the gap of the electromagnet so that the magnetic field $\vec{H}$ was directed tangentially to the YIG film and parallel to the rectilinear microstrip. This corresponded to the excitation geometry of magnetostatic surface waves [45].

The measurements were carried out according to the technique described in [40–43]. The frequency dependences of the electromotive forces $V(f)$ obtained upon excitation of magnetostatic surface waves by a focusing (Fig. 1, *c*) and rectilinear (Fig. 1, *b*) transducers were compared. Due to the nonreciprocity of propagation of magnetostatic surface waves, it was necessary to change the direction of the magnetic field $\vec{H}$ to the opposite along with the change of the input antenna, so that in both cases the magnetostatic surface waves propagated along the YIG/Pt interface.

2. Results and discussion

Fig. 2, *a* shows the frequency dependences of the transmission coefficient S_{12} measured at $P_{\text{in}} = -20$ dBm and $H = 939$ Oe in YIG/Pt structures, where one of the antennas has a curvilinear shape and focuses magnetostatic surface waves (curve *1*) and where both antennas are rectilinear (curve *2*). It can be seen from the figure that the amplitude of the magnetostatic surface wave signal transmitted through the model at frequencies $f < f^* \approx 4.9$ GHz in the case of excitation by the focusing antenna is higher by ≈ 8 dB than in the model with rectilinear antennas. This is due to the fact that focusing antennas of magnetostatic surface waves are characterized by chromatic aberration, which manifests itself in the dependence of the focal length of the antenna on the frequency [21]. In the frequency range $f < f^* \approx 4.9$ GHz, focusing prevents the spreading of the beam of the magnetostatic surface wave and most of its power reaches the output antenna. At frequencies $f > f^*$ the opposite situation occurs — better passage of the magnetostatic surface wave is observed for the case of a rectilinear antenna. This is due to the fact that as the frequency f increases, the focus position shifts toward the exciting antenna and the caustics, which carry a significant part of the power of the magnetostatic surface wave behind the focal point, bend around the output antenna (Fig. 3).

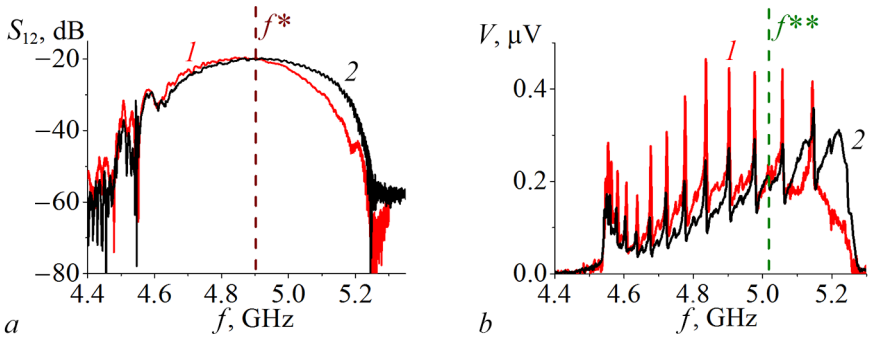

Fig 2. Results of the measurements of frequency dependencies of the transmission coefficient S_{12} (a) and EMF V (b) at $P_{\text{in}} = -20$ and -10 dBm respectively, where curves *1* and *2* correspond to the cases of MSSW excitation by focusing and straight antennas; frequency positions f^* in fig. a and f^{**} in fig. b, at which "equalization" of curves *1* and *2* happens, are shown by dash lines

Figures 2, b show the frequency dependences of the electromotive force V measured at $P_{\text{in}} = -10$ dBm in the YIG/Pt structure, where the excitation of the magnetostatic surface wave was carried out by focusing (curve *1*) or rectilinear (curve *2*) antennas. Note the oscillating nature of curves *1* and *2*. This is due to the van Hove singularities in the density of states $\eta(f)$ in the spectrum of the magnetostatic surface wave at the frequencies of dipole-exchange resonances and was discussed in more detail in [42]. It can be seen from the figure that at frequencies $f < f^{**} \approx 5.05$ GHz in the case of a focusing antenna the signal value V was 10–20 % greater than in the case of a rectilinear antenna. At the frequency f^{**} the V values of curves *1* and *2* were equalized, and at frequencies $f > f^{**}$ the electromotive force was greater in the case of a rectilinear antenna. To explain this behavior of the $V(f)$ dependence, let us refer to Fig. 3.

Figure 3 shows the results of micromagnetic simulation of two-dimensional maps of the Fourier amplitude distribution of the magnetostatic surface waves wave field in the XY plane in the vicinity of the focusing antenna (marked as 1) at frequencies $f = 4.65...4.9$ GHz and at $H = 960$ Oe, obtained using OOMMF [46]. The simulation was carried out according to the approach of [32] with parameters corresponding to the experiment. It can be seen from Figure 3 that the excitation of magnetostatic surface waves by a curvilinear antenna leads to the focusing of magnetostatic surface waves. At the same time, with increasing frequency f, the focus position

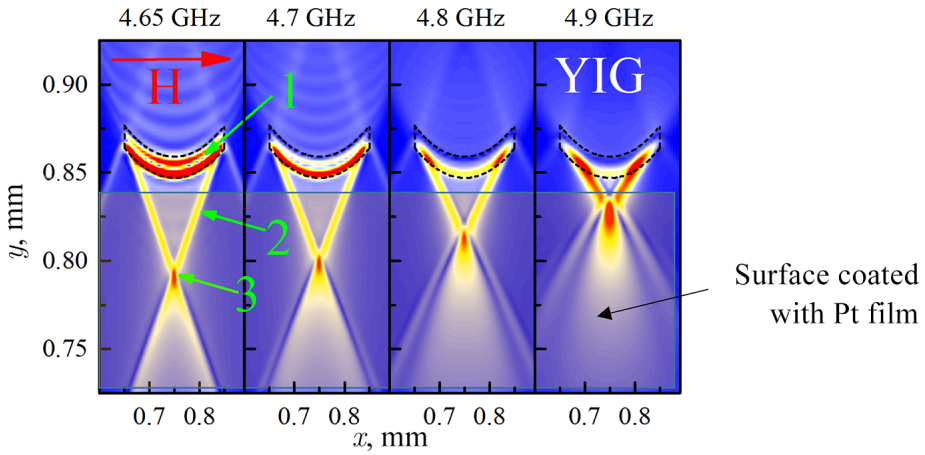

Fig 3. Distribution of Fourier-amplitude of MSSW field excited by focusing antenna (1) in XY plane at frequencies $f = 4.65...4.9$ GHz where 2 — formed caustics, 3 — position of MSSW focus (color online)

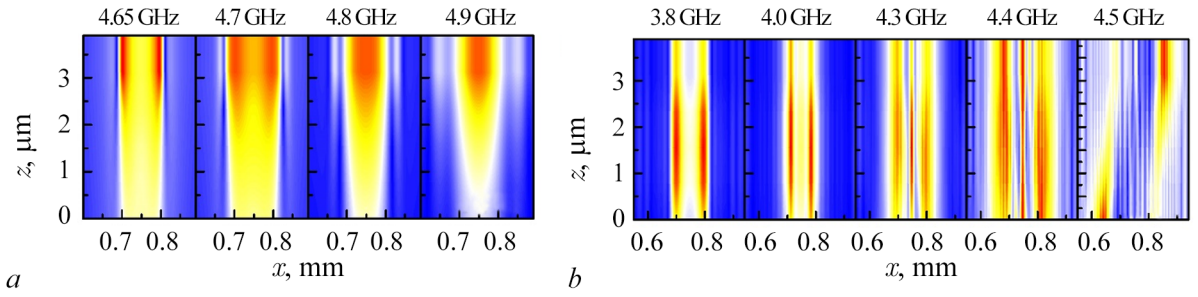

Fig 4. Distribution of Fourier-amplitude of MSSW (*a*) and BVMSW (*b*) field excited by focusing antenna in XZ plane (color online)

(marked as 3 in Figure 3) shifts closer to the focusing antenna, but remains on the Pt-coated YIG film section. At frequencies $f > 4.9$ GHz the focal position is between the antenna and the YIG film region coated with Pt. As the frequency of magnetostatic surface waves increases, the angle between the y-axis directions and the caustics (marked as 2 in Fig. 3) formed during focusing increases.

The propagation of caustics of magnetostatic surface waves formed at the antenna edges is mutual with respect to the optical axis of the antenna. This follows from the results of micromagnetic modeling of the propagation of a magnetostatic surface wave, the amplitude of which at several frequencies in the XZ plane of the YIG film cross-section is shown in Fig. 4, *a*. In the case of BVMSW, the nature of caustics propagation is fundamentally different. This can be seen from Fig. 4, *b*. The nonreciprocity is especially pronounced for the frequency $f = 4.5$ GHz. The distribution of the amplitudes of the "left"and "right"caustics with respect to the optical axis is nonreciprocal — the maxima of their amplitudes are near different surfaces of the YIG film.

Thus, the previously noted increase in the magnitude of the electromotive force signal at frequencies $f < f^{**}$ can be associated with two reasons: 1) with the formed caustics, which reflect the increase in the density of states $\eta(f)$ in the spectrum of magnetostatic surface waves, which is similar to the case of dipole-exchange resonances; 2) focusing of magnetostatic surface waves leads to an increase in the density of the linear power of magnetostatic surface waves, which is equivalent to the case of an increase in the input power level P_{in}.

Conclusion

The possibility of detecting focused beams of magnetostatic surface waves excited by a focusing curvilinear transducer using the inverse spin Hall effect is demonstrated using YIG/Pt structures. A comparison is made of the frequency dependences of the electromotive force $V(f)$ induced on the contacts to Pt under conditions of focusing of magnetostatic surface waves and under excitation by a rectilinear transducer. It is noted that the value of $V(f)$ generated by focused magnetostatic surface waves is significantly affected by the chromatic aberration of the focusing antenna. It is shown that focusing of magnetostatic surface waves leads to an increase in the electromotive force signal relative to the case of a rectilinear antenna at those frequencies $f < f^{**}$ at which the position of the focus of magnetostatic surface waves is located on the structure section covered with Pt. At frequencies $f > f^{**}$, at which the focus position is between the antenna and the YIG region coated with Pt, the electromotive force signal, on the contrary, decreases. The indicated increase in the electromotive force at frequencies $f < f^{**}$ can be associated with an increase in the linear power density of magnetostatic surface waves

and caustics formed during focusing, which reflect an increase in the density of states $\eta(f)$ in the spectrum of magnetostatic surface waves, which should lead to an increase in the processes of electron-magnon scattering.

References

1. Nikitov SA, Kaliabin DV, Lisenkov IV, Slavin AN, Barabanenkov YuN, Osokin SA, Sadovnikov AV, Beginin EN, Morozova MA, Sharaevskii YuP, Filimonov YA, Khivintsev YV, Vysotskii SL, Sakharov VK, Pavlov ES. Magnonics: a new research area in spintronics and spin wave electronics. Phys. Usp. 2015;58(10):1002–1028. DOI: 10.3367/UFNr.0185.201510m.1099.
2. Nikitov SA, Safin AR, Kalyabin DV, Sadovnikov AV, Beginin EN, Logunov MV, Morozova MA, Odintsov SA, Osokin SA, Sharaevskaya AYu, Sharaevsky YuP, Kirilyuk AI. Dielectric magnonics: from gigahertz to terahertz. Phys. Usp. 2020;63:945–974. DOI: 10.3367/UFNe.2019.07.038609.
3. Chumak AA, Vasyuchka VI, Serga AA, Hillebrands B. Magnon spintronics. Nature Phys. 2015;11:453. DOI: doi:10.1038/nphys3347.
4. Demidov VE, Urazhdin S, Loubens G, Klein O, Cros V, Anane A, Demokritov SO. Magnetization oscillations and waves driven by pure spin currents. Phys. Rep. 2017;673:1–31. DOI: 10.1016/j.physrep.2017.01.001.
5. Althammer M. Pure spin currents in magnetically ordered insulator/normal metal heterostructures. J. Phys. D: Appl. Phys. 2018;51:313001. DOI: 10.1088/1361-6463/aaca89.
6. Demidov VE, Urazhdin S, Anane A, Cros V, Demokritov SO. Spin–orbit-torque magnonics. Journal of Applied Physics. 2020;127(17):170901. DOI: 10.1063/5.0007095.
7. Brataas A., van Wees B., Klein O., de Loubens G., Viret M. Spin insulatronics. Physics Reports. 2020;885:1–27. DOI: 10.1016/j.physrep.
8. Mahmoud A, Ciubotaru F, Vanderveken F, Chumak AV, Hamdioui S, Adelmann C, Cotofana S. Introduction to spin wave computing. J. Appl. Phys. 2020;128(16):161101. DOI: 10.1063/5.0019328.
9. Chumak AV, Kabos P, Wu M, Abert C, Adelmann C, Adeyeye AO, Akerman J, Aliev FG, Anane A, Awad A, Back CH, Barman A, Bauer GEW, Becherer M, Beginin EN, Bittencourt VASV, Blanter YM, Bortolotti P., Boventer I, Bozhko DA, Bunyaev SA, Carmiggelt JJ, Cheenikundil RR, Ciubotaru F, Cotofana S, Csaba G, Dobrovolskiy OV, Dubs C, Elyasi M, Fripp KG, Fulara H, Golovchnsiy IA, Gonzalez-Ballster C, Graczyk P, Grundler D, Gruszecki P, Gubbiotti G, Guslienko K, Haldar A, Hamdioui S, Hertel R, Hillebrands B, Hioki T, Houshang A, Hu CM, Huebl H, Huth M, Iacocca E, Jungfleisch MB, Kakazei GN, Khitun A, Khymyn R, Kikkawa T, Klaui M, Klein O, Klos JW, Knauer S, Koraltan S, Kostylev M, Krawczyk M, Krivorotov IN, Kruglyak VV, Lachance-Quirion D, Ladak S, Lebrun R, Li Y, Linder M, Macedo R, Mayr S, Melkov GA, Mieszczak S, Nakamura Y, Nembach HT, Nikitin AA, Nikitov SA, Novosad V, Otalora JA, Otani Y, Papp A, Pigeau B, Pirro P, Porod W, Porrati F, Qin H, Rana B, Reimann T, Reinte F, Romero-Isart O, Ross A, Sadovnikov AV, Safin AR, Saitoh E, Schmidt G, Schultheiss H, Schultheiss K, Serga AA, Sharma S, Shaw JM, Suess D, Surzhenko O, Szulc K, Taniguchi T, Urbanek M, Usami K, Ustinov AB, van der Sar T, van Dijken S, Vasyuchka VI, Verba R, Kusminskiy SV, Wang Q, Weides M, Weiler M, Wintz S, Wolski SP, Zhang X. Advances in Magnetics Roadmap on Spin-Wave Computing. IEEE Transactions on Magnetics. 2022;58(6):0800172. DOI: 10.1109/TMAG.2022.3149664.
10. Khitun A. Magnonic holographic devices for special type data processing. J. Appl. Phys. 2013;113(16):164503. DOI: 10.1063/1.4802656.
11. Gertz F, Kozhevnikov A, Filimonov Y, Nikonov DE, Khitun A. Magnonic holographic

memory: From proposal to device. IEEE J.Explor. Solid-State Comput. Devices Circuits. 2015;1:67–75. DOI: 10.1109/JXCDC.2015.2461618.
12. Khivintsev Y, Ranjbar M, Gutierrez D, Chiang H, Kozhevnikov A, Filimonov Y, Khitun A. Prime factorization using magnonic holographic devices. J. Appl. Phys. 2016;120(12):123901. DOI: 10.1063/1.4962740.
13. Gutierrez D, Chiang H, Bhowmick T, Volodchenkov AD, Ranjbar M, Liu G, Jiang C, Warren C, Khivintsev Y, Filimonov Y, Garay J, Lake R, Balandin AA, Khitun A. Magnonic holographic imaging of magnetic microstructures. JMMM. 2017;428:348–356. DOI: 10.1016/j.jmmm.2016.12.022.
14. Papp A, Porod W, Csurgay AI, Csaba G. Nanoscale spectrum analyzer based on spin-wave interference. Sci. Rep. 2017;7:9245. DOI: 10.1038/s41598-017-09485-7.
15. Csaba G, Papp A, Porod W. Holographic Algorithms for On-Chip, Non-Boolean Computing. In: Proceedings of the 17th International Workshop on Computational Electronics (IWCE 2014). 2014, Paris, France. P. 33–34. DOI: 10.1109/IWCE.2014.6865814.
16. Csaba G, Papp A, Porod W. Perspectives of using spin waves for computing and signal processing. Phys. Lett. A. 2017;381:1471. DOI: 10.1016/j.physleta.2017.02.042.
17. Macia F, Kent AD, Hoppensteadt FC. Spin-wave interference patterns created by spin-torque nano-oscillators for memory and computation. Nanotechnology. 2011;22:095301. DOI: 10.1088/0957-4484/22/9/095301.
18. Csaba G., Papp A., Porod W. Spin-wave based realization of optical computing primitives. J. Appl.Phys. 2014;115(17):17C741. DOI: 10.1063/1.4868921.
19. Vogel M, Hillebrands B, von Freymann G. Spin-Wave Optical Elements: Towards Spin-wave Fourier Optics. arXiv:1906.02301v1 [physics.app-ph]
20. Papp A, Csaba G. Lens Design for Computing With Anisotropic Spin Waves. IEEE Magn. Lett. 2018;9:3706405. DOI: 10.1109/LMAG.2018.2872127.
21. Vashkovskii AV, Stalmakhov AV, Shakhnazaryan DG. Forming, reflection and refraction of magnetostatic waves beams. Soviet Physics Journal. 1988;31:908–915. DOI: 10.1007/BF00893543.
22. Davies CS, Kruglyak VV. Graded-index magnonics. Low Temperature Physics. 2015;41: 760–766. DOI: 10.1063/1.4932349.
23. Schneider T, Serga AA, Chumak AV, Sandweg CW, Trudel S, Wolff S, Kostylev MP, Tiberkevich VS, Slavin AN, Hillebrands B. Nondiffractive subwavelength wave beams in a medium with externally controlled anisotropy. Phys. Rev. Lett. 2010;104:197203. DOI: 10.1103/PhysRevLett.104.197203.
24. Ulrichs H, Demidov VE, Demokritov SO, Urazhdin S. Spin-torque nano-emitters for magnonic applications. Appl. Phys. Lett. 2012;100:162406. DOI: 10.1063/1.4704563.
25. Gieniusz R, Ulrichs H, Bessonov VD, Guzowska U, Stognii AI, Maziewski A. Single antidot as a passive way to create caustic spin-wave beams in yttrium iron garnet films. Appl. Phys. Lett. 2013;102:102409. DOI: 10.1063/1.4795293
26. Gieniusz R, Bessonov VD, Guzowska U, Stognii AI, Maziewski A. An antidot array as an edge for total non-reflection of spin waves in yttrium iron garnet films. Appl. Phys. Lett. 2014;104(8):082412. DOI: 10.1063/1.4867026.
27. Mansfeld S, Topp J, Martens K, Toedt JN, Hansen W, Heitmann D, Mendach S. Spin Wave Diffraction and Perfect Imaging of a Grating. Phys. Rev. Lett. 2012;108:047204. DOI: 10.1103/PhysRevLett.108.047204.
28. Choi S, Lee KS, Kim SK. Spin-wave interference. Appl. Phys. Lett. 2006;89(6):062501. DOI: 10.1063/1.2259813.
29. Gruszecki P, Kasprzak M, Serebryannikov AE, Krawczyk M, Śmigaj W. Microwave excita-

tion of spin wave beams in thin ferromagnetic films. Sci. Rep. 2016;6: 22367. DOI: 10.1038/srep22367.
30. Körner HS, Stigloher J, Back CH. Excitation and tailoring of diffractive spin-wave beams in NiFe using nonuniform microwave antennas. Phys. Rev. B. 2017;96:100401(R). DOI: 10.1103/PhysRevB.96.100401.
31. Loayza N, Jungfleisch MB, Hoffmann A, Bailleul M, Vlaminck V. Fresnel diffraction of spin waves. Phys. Rev. B. 2018;98:144430. DOI: 10.1103/PhysRevB.98.144430.
32. Madami M, Khivintsev Y, Gubbiotti G, Dudko G, Kozhevnikov A, Sakharov V, Stal'makhov A, Khitun A, Filimonov Y. Nonreciprocity of backward volume spin wave beams excited by the curved focusing transducer. Appl. Phys. Lett. 2018;113(15):152403. DOI: 10.1063/1.5050347.
33. Kajiwara Y, Harii K, Takahashi S, Ohe J, Uchida K, Mizuguchi M, Umezawa H, Kawai H, Ando K, Takanashi K, Maekawa S, Saitoh E. Transmission of electrical signals by spin-wave in-ter-conversion in a magnetic insulator. Nature. 2010;464:262–266. DOI: 10.1038/nature08876.
34. Collet M, de Milly X, d'Allivy Kelly O, Naletov VV, Bernard R, Bortolotti P, Ben Youssef J, Demidov VE, Demokritov SO, Prieto JL, Muñoz M, Cros V, Anane A, de Loubens G, Klein O. Generation of coherent spin-wave modes in yttrium iron garnet microdiscs by spin–orbit torque. Nat Commun. 2016;7:10377. DOI: 10.1038/ ncomms10377.
35. Uchida KI, Adachi H, Ota T, Nakayama H, Maekawa S, Saitoh E. Observation of longitudinal spin-Seebeck effect in magnetic insulators. Appl. Phys. Lett. 2010;97(17):172505. DOI: 10.1063/1.3507386.
36. Chumak AV, Serga AA, Jungfleisch MB, Neb R, Bozhko DA, Tiberkevich VS, Hillebrands B. Direct detection of magnon spin transport by the inverse spin Hall effect. Appl. Phys. Lett. 2012;100(8):082405. DOI: 10.1063/1.3689787.
37. d'Allivy Kelly O, Anane A, Bernard R, Ben Youssef J, Hahn C, Molpeceres AH, Carrétéro C, Jacquet E, Deranlot C, Bortolotti P, Lebourgeois R, Mage JC, de Loubens G, Klein O, Cros V, Fert A. Inverse spin Hall effect in nanometer-thick yttrium iron garnet/Pt system. Appl. Phys. Lett. 2013;103(8):082408. DOI: 10.1063/1.4819157 .
38. Balinsky M, Ranjbar M, Haidar M, Dürrenfeld P, Dumas RK, Khartsev S, Slavin A, Åkerman J. Spin pumping and the inverse spin Hall effect via magnetostatic surface spin-wave modes in YIG/Pt bilayers. IEEE Magn. Lett. 2015;6:3000604. DOI: 10.1109/LMAG.2015.2471276.
39. Balinsky M, Chiang H, Gutierrez D, Khitun A. Spin wave interference detection via inverse spin Hall effect. Appl. Phys. Lett. 2021;118(24): 242402. DOI: 10.1063/5.0055402.
40. Seleznev ME, Nikulin YV, Khivintsev YV, Vysotskii SL, Kozhevnikov AV, Sakharov VK, Dudko GM, Pavlov ES, Filimonov YA. Influence of three-magnon decays on electromotive force generation by magnetostatic surface waves in integral YIG – Pt structures. Izvestiya VUZ. Applied Nonlinear Dynamics. 2022;30(5):617–643. DOI: 10.18500/0869-6632-003008.
41. Seleznev ME, Nikulin YV, Sakharov VK, Khivintsev YV, Kozhevnikov AV, Vysotskii SL, Filimonov YA. Influence of the resonant interaction of surface magnetostatic waves with exchange modes on the EMF generation in YIG/Pt structures. Technical Physics. 2022; 92(13):2074–2077. DOI: 10.21883/TP.2022.13.52224.136-21.
42. Seleznev ME, Nikulin YV, Khivintsev YV, Vysotskii SL, Kozhevnikov AV, Sakharov VK, Dudko GM, Filimonov YA. Influence of parametric instability on spin pumping by dipole-exchange magnetostatic surface waves in YIG–Pt structures. Izvestiya VUZ. Applied Nonlinear Dynamics. 2023;31(2):225–242. DOI: 10.18500/0869-6632-003032.

43. Nikulin YV, Vysotskii SL,Seleznev ME, Kozhevnikov AV, Sakharov VK, Dudko GM, Khivintsev YV, Filimonov YA. Frequency dependence of the spin mixing conductance of YIG/Pt structures upon MSSW spin pumping. Phys. Solid State. 2023;65(6):926–931. DOI: 10.21883/PSS.2023.06.56103.10H.
44. Dudko GM, Kozhevnikov AV, Saharov VK, Stalmahov AV, Filimonov YA, Khivintsev YV. Calculation of Focusing Spin Wave Transducers Using the Method of Micromagnetic Simulation. Izvestiya of Saratov University. Physics. 2018;18(2):92–102. DOI: 10.18500/1817-3020-2018-18-2-92-102.
45. Damon R, Eshbach J. Magnetostatic modes of a ferromagnetic slab. J. Phys.Chem. Sol. 1961;(3–4):308–320. DOI: 10.1016/0022-3697(61)90041-5.
46. Donahue MJ, Porter DG. OOMMF user's guide, version 1.0. Interagency Report NIST 6376. National Institute of Standards and Technology, Gaithersburg, MD, 1999. DOI: 10. 6028/NIST.IR.6376.